


SCIENTIFIC REPORTS



OPEN

Layered transition metal dichalcogenides: promising near-lattice-matched substrates for GaN growth

Received: 04 December 2015

Accepted: 10 March 2016

Published: 30 March 2016

Priti Gupta¹, A. A. Rahman¹, Shruti Subramanian¹, Shalini Gupta^{1,2}, Arumugam Thamizhavel¹, Tatyana Orlova³, Sergei Rouvimov³, Suresh Vishwanath³, Vladimir Protasenko³, Masihur R. Laskar⁴, Huili Grace Xing³, Debdeep Jena³ & Arnab Bhattacharya¹

Most III-nitride semiconductors are grown on non-lattice-matched substrates like sapphire or silicon due to the extreme difficulty of obtaining a native GaN substrate. We show that several layered transition-metal dichalcogenides are closely lattice-matched to GaN and report the growth of GaN on a range of such layered materials. We report detailed studies of the growth of GaN on mechanically-exfoliated flakes WS₂ and MoS₂ by metalorganic vapour phase epitaxy. Structural and optical characterization show that strain-free, single-crystal islands of GaN are obtained on the underlying chalcogenide flakes. We obtain strong near-band-edge emission from these layers, and analyse their temperature-dependent photoluminescence properties. We also report a proof-of-concept demonstration of large-area growth of GaN on CVD MoS₂. Our results show that the transition-metal dichalcogenides can serve as novel near-lattice-matched substrates for nitride growth.

The group-III nitride semiconductors¹ — GaN, AlN, InN and their alloys — are important materials for compact, energy-efficient, solid-state lighting sources as well as ideal candidates for high-power²/high-temperature³ electronic devices. There have been phenomenal improvements in the performance of GaN-based LEDs^{4,5}, laser diodes⁶, and transistors⁷; however, a fundamental challenge in these materials has been the extreme difficulty of obtaining a native GaN substrate compelling the use of non-lattice-matched substrates like sapphire or silicon^{8–10}. While breakthroughs^{11,12} in epitaxial growth techniques have dramatically improved material quality on sapphire, there has always been a quest to seek lattice-matched substrate materials for GaN growth. In this work, we show that several layered transition metal dichalcogenides¹³ are closely lattice matched to GaN and report the metalorganic vapour phase epitaxial (MOVPE) growth of GaN on a range of such layered materials. In particular, we show WS₂ and MoS₂ to be promising substrates for III-nitride growth.

The past few years have seen a frenzy of activity in research in 2-dimensional layered materials, motivated by the exceptional properties of graphene¹⁴ and the demonstration of a range of novel devices. The transition-metal dichalcogenides (TMDCs)¹³ — layered materials analogous to graphene but which also offer a bandgap¹⁵ — have been a subject of great recent interest due to their own unique electrical and optical properties. Most of the work in semiconducting layered materials has focused on their potential for opto-electronic devices^{16–20}. What has perhaps not been noticed is their relatively close in-plane lattice match with materials of the III-nitride family. Figure 1 shows the bandgap versus in-plane lattice parameter for different III-nitrides and TMDCs. WS₂ and MoS₂ have a lattice mismatch of only 1.0% and 0.8%, respectively to the ‘a’ lattice parameter of GaN. Further, the weak out-of-plane (van der Waal’s) interactions and absence of dangling bonds on the surface of the layered chalcogenides may help in controlling stress between the nitride layer and substrate. The TMDCs can thus not only provide novel near-lattice-matched substrates for nitride growth, but also likely to allow the study of novel heterostructures in combination with the III-nitride materials.

¹Department of Condensed Matter Physics and Materials Science, Tata Institute of Fundamental Research, Mumbai, India. ²UM-DAE Center for Excellence in Basic Sciences, Mumbai, India. ³Department of Electrical Engineering, University of Notre Dame, Notre Dame, USA. ⁴Department of Chemical and Biological Engineering, University of Wisconsin-Madison, USA. Correspondence and requests for materials should be addressed to A.B. (email: arnab@tifr.res.in)

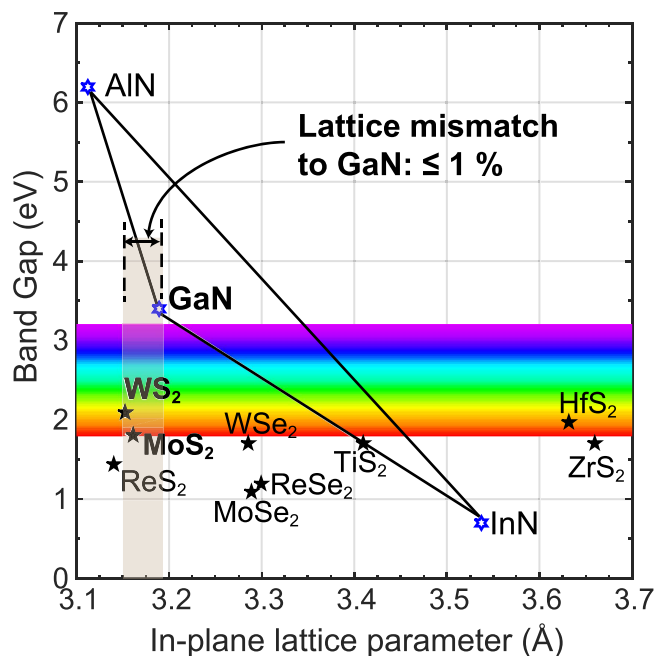


Figure 1. Band gap versus in-plane lattice parameter for different III-nitrides and TMDCs. The lattice mismatch of WS_2 and MoS_2 with respect to GaN are 1.0% and 0.8%, respectively. Supplementary information section S1 lists the sources from where the lattice parameters and bandgaps of different III-nitrides and TMDCs materials were obtained.

Results and Discussion

To test their viability as substrates for nitride growth, mechanically-exfoliated flakes of the layered TMDCs were transferred to SiO_2 (300 nm thick) coated silicon wafers (details in supplementary information section S2). We chose SiO_2 -coated Si rather than sapphire, Si or SiC to minimize parasitic growth outside the flakes which may hinder the characterization of the GaN layer. In addition, for a proof-of-concept demonstration of large-area growth, CVD MoS_2 films synthesized by the sulphurization of thin Mo layers were used (details in supplementary information sections S2 and S3).

The heat-up procedure, carrier gas, nucleation conditions, growth temperature and V/III ratio were varied to determine the optimal conditions for growth of GaN on WS_2 and MoS_2 . The MOVPE growth of GaN typically occurs at a high temperature, $>1000^\circ\text{C}$, in an ambient of ammonia and hydrogen, rather aggressive conditions, which are in some cases close to the thermal decomposition temperatures of the chalcogenide materials. This makes the procedure for initiation of growth on the TMDC material very critical, especially the choice of carrier gas and temperature ramp during the heat-up procedure, and the conditions for the growth of the nucleation layer. Our observations suggest that ramping up to the growth temperature is best done using nitrogen (N_2) as a carrier gas to preserve the integrity of the TMDC layer (a detailed study of thermal annealing of MoS_2 and WS_2 in different ambients is presented in supplementary information section S4). We switch the carrier gas to hydrogen just before the growth of the GaN layer, and again cool down to room temperature under N_2 . Based on optimization experiments, we have used a short initial GaN nucleation layer grown at 900°C for 40 s at a V/III ratio of ~ 1400 , following which a second layer is grown at the more usual growth temperature of 1040°C at a V/III ratio of ~ 2100 (we will refer this second layer growth time as t_{GaN}). The low temperature GaN layer also ensures the conformal coverage of GaN on the TMDC substrate.

Growth of GaN on WS_2 . We first discuss the growth of GaN on WS_2 . For $t_{\text{GaN}} = 300$ s, nearly hexagonal crystals of GaN are obtained only on WS_2 flakes as shown in Fig. 2(a,b). From the XRD profile of GaN on WS_2 (Fig. 2(c)), it is clearly seen that GaN is growing in the (0002) direction as expected. The few stray peaks are possibly due to either random nucleation on SiO_2/Si or due to growth on mis-oriented WS_2 flakes stamped on the substrate. All the GaN/ WS_2 flakes are oriented in (0002) direction as confirmed from the large area electron back scattering diffraction (EBSD) map (Fig. 2(e)). A detailed EBSD map of one flake (Fig. 2(d)), shows that the GaN is single crystal with no grain boundary. Similar EBSD maps on several other flakes confirm the single crystal growth of GaN on WS_2 . The observation of a (0002) oriented GaN layer is not surprising. Even if there are no bonds across the interface, the atomic arrangement of the underlying layer would still influence the energy landscape on the growth surface and hence have an effect on the nucleation and growth of the epilayer. Thus, the lattice structure of the substrate will influence the epitaxial relation. For closely-lattice-matched systems, as in the case of the TMDCs, the substrate's lattice points will be the energetically favoured regions and the little strain that may arise from a small mismatch is easily relaxed because of the absence of strong interlayer bonding. The lattice parameters of GaN were calculated from the (0002) and (10 $\bar{1}$ 1) peak positions in the powder XRD scan. The obtained value of the in-plane lattice parameter was 3.19 \AA which is almost equal to that reported for unstrained

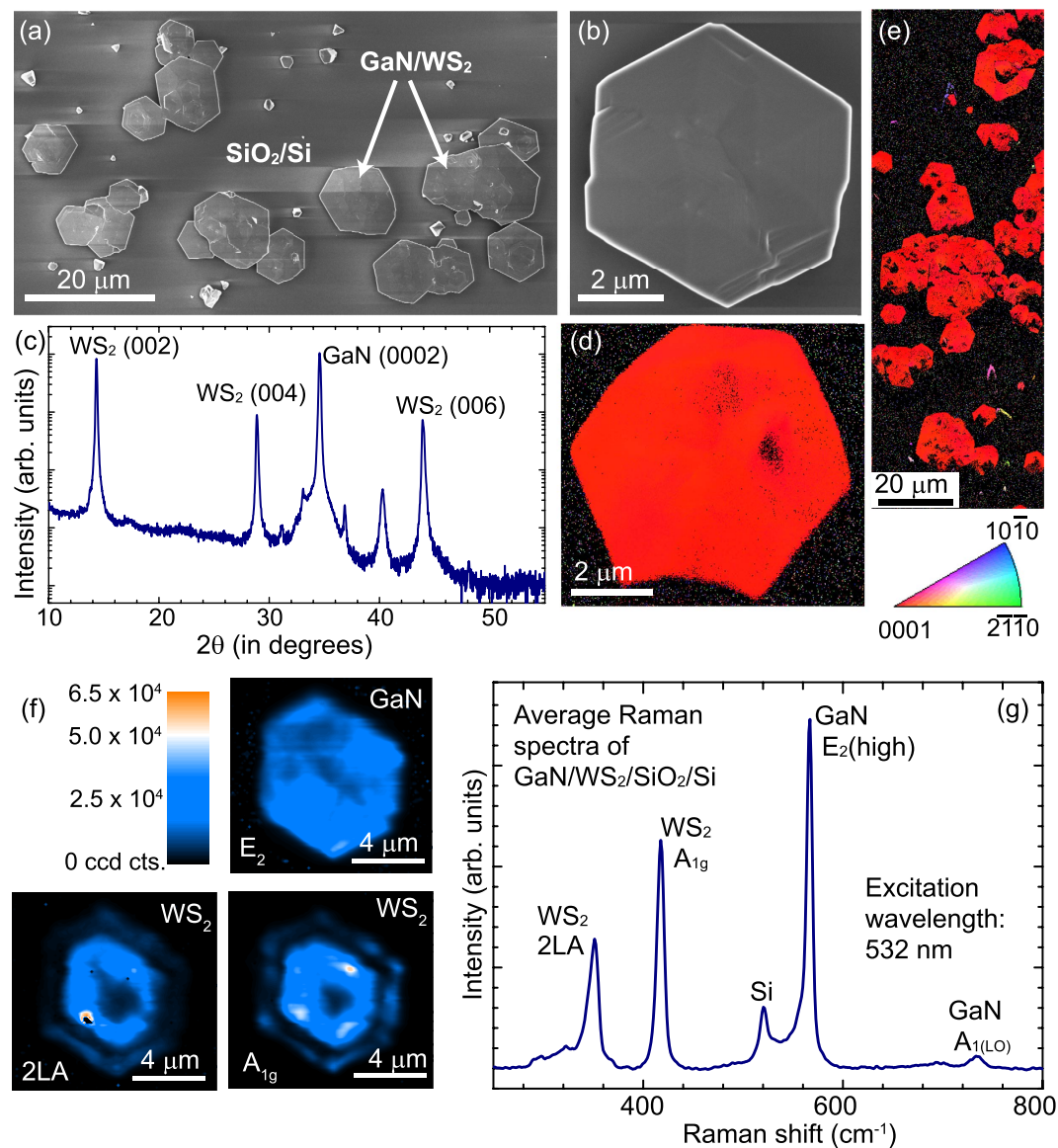


Figure 2. Growth of GaN on exfoliated WS₂ flakes. (a) Scanning electron microscopy confirms near-hexagonal crystals of GaN growing only in the region covered by the WS₂ flakes. (b) Micrograph showing single hexagonal crystal of GaN grown on WS₂ (c) X-ray diffraction profile of GaN on WS₂ shows preferential (0002) orientation. (d,e) EBSD maps of GaN grown on exfoliated WS₂ clearly show that the grown GaN layer is single crystal and (0002) oriented. (f) Integrated Raman mapping over an area of 10 μm × 11 μm for the intensity of following Raman modes E₂(high) of GaN, 2LA and A_{1g} mode of WS₂. The colour scale is based on the intensity of the GaN E₂(high) mode. Fig. S2 in the supplementary information shows the WS₂ feature in greater detail confirming its presence everywhere below the GaN layer. (g) Spatially averaged Raman scattering spectrum of GaN/WS₂ over the flake shown in (f) shows the survival of WS₂ after growth and the peak position of E₂(high) indicates that GaN layer on WS₂ is strain-free.

GaN i.e. 3.189 Å. Thus, as expected, the GaN layer being grown on a closely-lattice matched substrate is almost strain-free.

Raman spectroscopy was used to examine the residual stress and to monitor the quality of the GaN layer. The frequency shift of the strongest phonon mode E₂(high) is very sensitive to the residual stress^{21,22} whereas the width depends on the quality of the layer²². The lattice- and thermal-mismatch between the layer and the substrate result in a residual strain which is usually compressive for GaN grown on sapphire, and tensile for GaN on Si²³. The E₂(high) mode of strain-free GaN is known to be at 566.2 cm⁻¹ at room temperature²¹, and shifts to higher frequency with compressive strain whereas a downshift indicates tensile strain. Figure 2(f) shows the Raman integrated maps of the E₂(high) mode of GaN, and 2LA and A_{1g} modes of WS₂. These maps clearly show the hexagonal-shaped islands of GaN grown on the underlying WS₂ with their edges being parallel to each other. The spatial extent of the GaN may be larger than the underlying WS₂ flake due to lateral overgrowth at the edges. The homogeneous intensity distribution of the E₂(high) peak also points to the uniform GaN growth over the

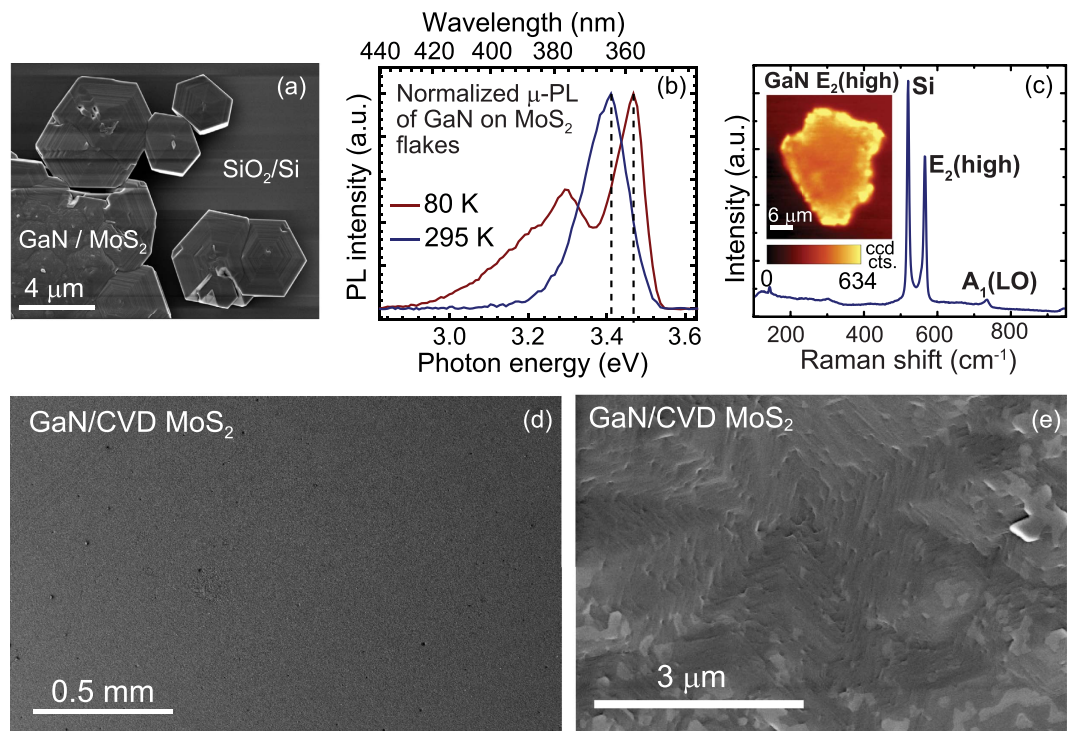


Figure 3. Growth of GaN on MoS₂. (a) Hexagonal crystals of GaN which are obtained only on MoS₂ flakes (b) Room- and low- temperature μ - photoluminescence spectra showing strong near-band-edge emission from the GaN (c) Spatially averaged Raman spectrum over GaN/MoS₂ flake (inset shows the integrated Raman map for the intensity of E₂(high) phonon mode of GaN). (d,e) SEM images showing the extension of GaN growth to large area CVD MoS₂.

WS₂ flake. The spatially-averaged Raman spectrum of GaN/WS₂ over a 10 $\mu\text{m} \times 11 \mu\text{m}$ area is shown in Fig. 2(g). The E₂ phonon peak for GaN/WS₂ is observed at 566.4 cm⁻¹ which is almost near the value reported for the unstrained GaN. This also confirms that the GaN layer grown on WS₂ is nearly strain-free. The linewidth of the E₂(high) peak is 6 cm⁻¹, comparable with that of (0002)-oriented GaN of similar thickness grown on sapphire with the standard two-temperature recipe.

Growth of GaN on MoS₂. Following a similar recipe, GaN layers were grown on MoS₂ as well. While one group had reported the molecular beam epitaxial growth of GaN on bulk MoS₂ in the 1990s^{24,25}, there has been no systematic study. GaN layers were deposited on exfoliated MoS₂ using MOVPE and again nearly hexagonal-shaped crystals of GaN are obtained only on the MoS₂ flakes. A typical SEM image of the surface is shown in Fig. 3(a). The GaN layer shows strong near-band-edge luminescence in room- and low-temperature photoluminescence (PL) (Fig. 3(b)). The details of PL are discussed later. Once again, the peak shift of the E₂(high) Raman mode is very small indicating nearly strain-free GaN on MoS₂ (Fig. 3(c)). The EBSD map of GaN grown on exfoliated MoS₂ (supplementary information section S5) also shows that grown GaN layer is single crystal similar to GaN grown on WS₂ and oriented in (0002) direction. From the low magnification and a zoomed-in SEM image of GaN grown on large area CVD MoS₂ (Fig. 3(d,e)), it is clear that there is conformal coverage across the substrate and this method is scalable to larger substrate sizes.

The GaN layers grown on exfoliated MoS₂ are preferentially oriented in (0002) direction as seen from XRD pattern in Fig. 4(a) (the XRD profile of GaN growth on CVD MoS₂ is very similar to that grown on exfoliated MoS₂, and is shown in supplementary information section S6). However, the surprising observation is that there are no characteristic MoS₂ peaks after the MOVPE growth (Fig. 4(a,b)). This suggests that the MoS₂ may have degraded under the MOVPE growth conditions (high growth temperature and exposure to ammonia and hydrogen). TEM imaging was used to confirm this hypothesis. As seen in Fig. 4(c), clear lattice fringes of the GaN layer are present in the top of the image. However, below the GaN, instead of the characteristic signature of layered MoS₂, only metallic molybdenum (Mo) was detected. A simple experiment to check the role of MoS₂ in the growth of GaN was to attempt to grow GaN on Mo metal alone using sputtered Mo layers deposited on sapphire. As seen in Fig. 4(d), faceted chunks of GaN were obtained and there was no conformal growth of GaN on Mo. The morphology of the Mo surface also changed after the MOVPE growth of GaN on Mo (Fig. 4(e,f)). This suggests that the MoS₂ was indeed present and served as a substrate for the initial growth of the GaN layer, but degraded at some point during the high temperature growth.

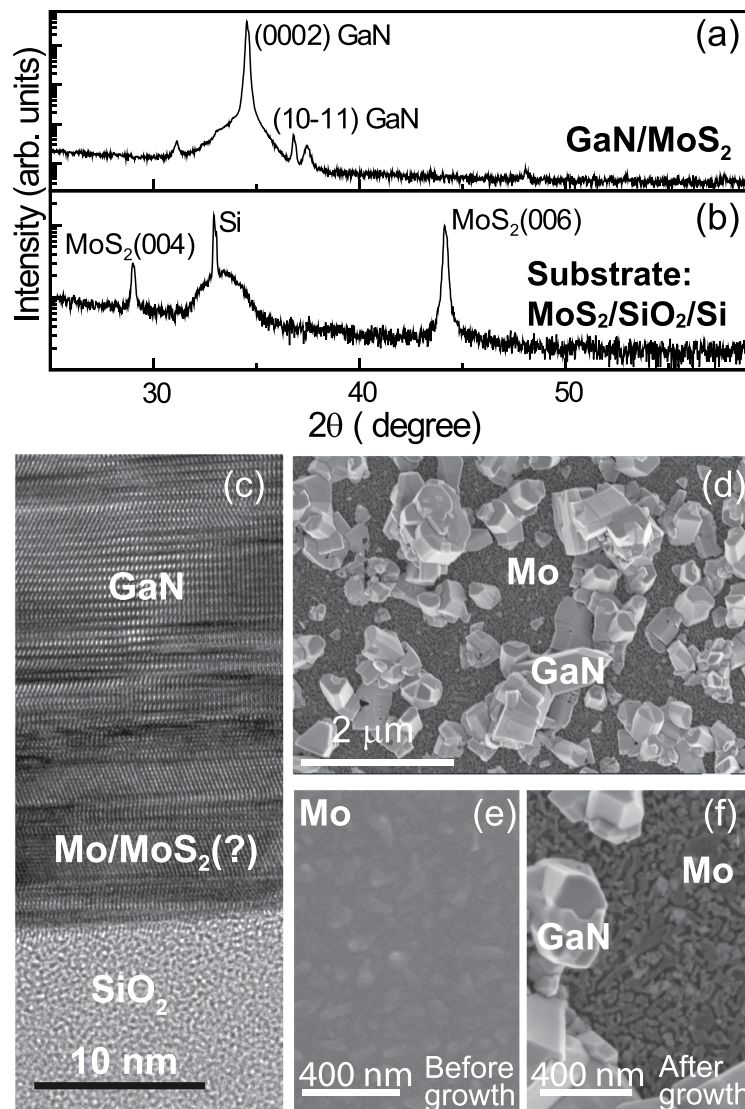


Figure 4. Necessity of MoS₂ for GaN growth. (a) X-ray diffraction profile of GaN on MoS₂ shows preferential (0002) orientation but no MoS₂ peak after growth as compared to substrate XRD profile (b). (c) Cross-sectional transmission electron micrograph does not show MoS₂ at the interface of substrate and GaN layer. (d) The SEM shows faceted chunks of GaN on Mo substrate and no conformal coverage of GaN. The micrographs below (d) show sputtered Mo on sapphire before (e) and after (f) growth.

Comparative photoluminescence spectroscopy of GaN grown on WS₂ and MoS₂. Temperature-dependent photoluminescence measurements were done on both the GaN/WS₂ and GaN/MoS₂ samples as shown in Fig. 5(a,b). The PL spectra exhibit a dominant near-band-edge (NBE) transition band at 3.41 eV (temperature (T) = 290 K), which clearly blue-shifts with decreasing temperature. Apart from this, there are two additional peaks at lower energies at 3.27 eV and 3.18 eV which we label as P1 and P2, respectively. We first discuss the behaviour of the NBE emission. The insets of Fig. 5(a,b) show the variation of NBE peak position with temperature which are fitted by the Bose-Einstein expression²⁶:

$$E(T) = E(0) - 2a_B / [\exp(\theta/T) - 1] \quad (1)$$

where $E(0)$ is the transition energy at $T = 0$ K and a_B is the strength of the average exciton-phonon interaction and θ is the average phonon frequency. The values of $E(T)$, a_B and θ as obtained from the fitted curves (with 95% confidence bounds) are shown in Table 1 and are in close agreement with the reported values for this temperature range²⁷. The $E(0)$ values obtained for the GaN grown on WS₂ and MoS₂ are 3.468 ± 0.002 eV and 3.469 ± 0.002 eV, respectively, very close to 3.471 eV²⁸ for unstrained GaN, again indicating strain-free layers.

The FWHM of the NBE emission line increases with increasing temperature due to increasing exciton-phonon interaction at higher temperatures. The temperature dependence of the linewidth has the usual form²⁹:

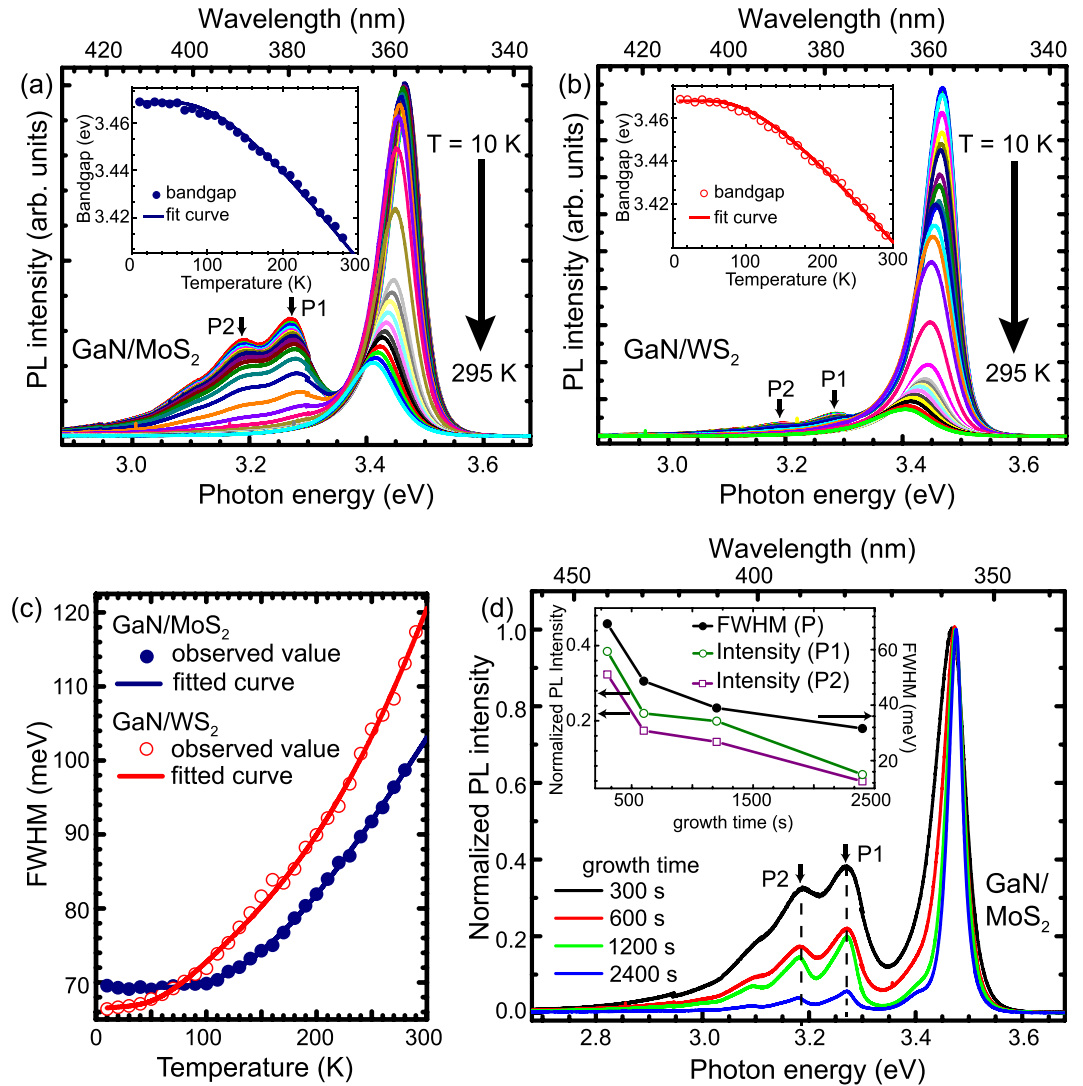


Figure 5. Comparative PL spectroscopy of GaN grown on WS₂ and on MoS₂. Temperature dependent photoluminescence of GaN grown (a) on WS₂ and (b) on MoS₂. Insets of (a,b) show the Bose-Einstein expression fit for the variation of NBE peak positions with temperature. (c) Temperature dependence of FWHM of NBE emission line for GaN/WS₂ and GaN/MoS₂. (d) Low temperature (10 K) PL of GaN grown on MoS₂ with different t_{GaN} (inset shows that intensity of peaks P1 and P2 decreases and NBE emission linewidth decreases with increasing t_{GaN}).

$$\Gamma(T) = \Gamma_{\text{inh}} + \gamma_{\text{LA}}T + \frac{\Gamma_{\text{LO}}}{\exp(\hbar\omega_{\text{LO}}/k_{\text{B}}T) - 1} + \Gamma_i \exp\left(-\frac{E_i}{k_{\text{B}}T}\right) \quad (2)$$

where Γ_{inh} is the inhomogeneous broadening term, γ_{LA} is a coefficient of exciton-acoustic-phonon interaction, Γ_{LO} is the exciton-LO-phonon coupling constant, ω_{LO} is the LO-phonon energy, Γ_i is a proportionality factor which accounts for the concentration of impurity centers and E_i is the binding energy of impurity-bound excitons averaged over all possible locations of the impurities. The obtained value of Γ_i from the fit curves for WS₂ and MoS₂ (Fig. 5(c)) are 55 ± 16 meV and 171 ± 87 meV, respectively which indicates that the concentration of impurity centers in GaN grown on WS₂ is lesser than that for the GaN grown on MoS₂. The same is also evident from the value of E_i which is lesser in case of GaN/WS₂ compared to that for GaN/MoS₂ (Table 1).

The peak intensity of P1 and P2 is larger in GaN/MoS₂ layer compared to GaN/WS₂ layer, which strongly suggests that these peaks arise from the defects originating from the degradation of the substrate. To confirm this hypothesis, GaN layers of different thicknesses were grown on MoS₂ ($t_{\text{GaN}} = 300$ s, 600 s, 1200 s and 2400 s). The low temperature (T = 10 K) PL spectra for these samples, normalized to the NBE peak, are shown in Fig. 5(d). It can be seen that on increasing t_{GaN} , i.e. with larger thickness of the GaN layer, the intensity of P1 and P2 decreases (inset of Fig. 5(d)). At our laser excitation energy the absorption length in GaN is only ~50–60 nm, hence the PL observed is mainly from the top ~200 nm GaN layer. The decrease in intensity of P1 and P2 thus indicates that the defect density in the

GaN/substrate	E(0) (eV)	a_B (meV)	θ (K)	Γ_i (meV)	E_i (meV)
GaN/WS ₂	3.468 ± 0.002	78 ± 18	365 ± 48	55 ± 16	20 ± 5
GaN/MoS ₂	3.469 ± 0.002	87 ± 24	385 ± 56	171 ± 87	46 ± 9

Table 1. The parameters E(0), a_B , θ , Γ_i and E_i of GaN layers grown on WS₂ and MoS₂ (with 95% confidence bounds).

top GaN layer reduces as the thickness increases. While this could be attributed to an overall reduction in extended defects, we believe that in our samples, P1 and P2 are related to point defects that originate from the GaN/substrate interface due to MoS₂ degradation. This was confirmed from the secondary ion mass spectrometry (SIMS) profile which showed a significant concentration of sulphur in the GaN layer (supplementary information section S7). Also, the FWHM of GaN/MoS₂ decreases on increasing t_{GaN} (the inset of Fig. 5(d)), indicating better GaN quality on increasing thickness. However, we have not found luminescence of sulphur impurities in GaN reported in literature.

GaN grown on other TMDCs. GaN growth on other mechanically-exfoliated TMDCs like WSe₂, MoSe₂, ReS₂ and ReSe₂ (lattice mismatch to GaN – ~1–3%) was also attempted (SEM images in supplementary information section S8). The micrographs clearly indicate that growth of GaN layer is possible on these substrates. However the heat-up and the growth initiation steps would need to be optimized for the different TMDCs keeping in mind their thermal stabilities and reactivities. With the proper optimization of MOVPE growth conditions, these TMDCs can also be potential substrates for III-nitride growth.

Conclusion

In conclusion, we report the MOVPE growth of strain-free, single-crystal islands of GaN on mechanically-exfoliated flakes of WS₂ and MoS₂, discussing their structural and optical properties. We also present a detailed comparison of temperature-dependent PL of GaN grown on WS₂ and MoS₂ and a preliminary demonstration of large-area growth of GaN on CVD MoS₂. Our investigations establish TMDCs as interesting near-lattice-matched substrates for GaN. With appropriate choice of substrates and growth conditions, it opens up the prospect of combining the III-nitrides with the transition metal dichalcogenides to realize novel heterostructures such as stacked layered MoS₂ and nitrides for solar energy conversion, as theoretically predicted³⁰ recently. Further, growth on large-area single crystal TMDCs may provide a route to large-area single crystal GaN layers which could be released to serve as bulk substrates.

Methods

Preparation of substrates. All the TMDCs were synthesized by first reacting the constituent elements in stoichiometric ratio to form precursors followed by iodine vapour transport in order to get bulk crystals suitable for exfoliation into thin films (details in supplementary information section S2). In the case of MoS₂, we used naturally available bulk MoS₂ crystals for exfoliation. Raman spectroscopy details of the exfoliated and CVD grown MoS₂, and exfoliated WS₂ substrate materials are provided in supplementary information section S3.

Growth of GaN layer. GaN layers were deposited on these TMDC substrates using low pressure MOVPE in a 3 × 2" close-coupled showerhead system using standard trimethylgallium (TMGa) and NH₃ precursors. H₂ carrier gas was used for the GaN layer growth with samples being heated up and cooled down using N₂ carrier gas. Based on a few flakes that we have studied (these are naturally a random selection) either via electron microscopy or SIMS, the growth rate of GaN layer on MoS₂ is approximately 50–70 nm per minute.

Characterization techniques. The films were structurally characterized using field-emission scanning electron microscopy (FE-SEM), X-ray diffraction (XRD), transmission electron microscopy (TEM) and electron back scattering diffraction (EBSD). The optical properties were measured by photoluminescence (PL) spectroscopy. Temperature-dependent PL measurements were done in the 10 K–295 K range using a set-up with a frequency-quadrupled 266 nm Nd:YAG laser for excitation, and a 0.55 m monochromator equipped with a cooled Si-CCD detector. Confocal Raman spectroscopy measurements were performed on the samples using 532 nm laser excitation. The Raman peak shift and the full width half maxima (FWHM) are determined by fitting a Lorentzian function to the observed data. For comparing the peak positions, the spectrum is aligned with reference to the Si substrate peak (520 cm⁻¹).

References

- Ambacher, O. Growth and applications of group III-nitrides. *J. Phys. D: Appl. Phys.* **31**, 2653 (1998).
- Baliga, B. J. Gallium nitride devices for power electronic applications. *Semicond. Sci. Technol.* **28**, 074011 (2013).
- Neudeck, P. G., Okojie, R. S. & Chen, L.-Y. High-temperature electronics—a role for wide bandgap semiconductors? *Proc. IEEE* **90**, 1065–1076 (2002).
- Wierer, J. J., David, A. & Megens, M. M. III-nitride photonic-crystal light-emitting diodes with high extraction efficiency. *Nature Photon.* **3**, 163–169 (2009).
- Ponce, F. & Bour, D. Nitride-based semiconductors for blue and green light-emitting devices. *Nature* **386**, 351–359 (1997).
- Arafin, F., Liu X. & Mi, Z. Review of recent progress of III-nitride nanowire lasers. *J. Nanophotonics* **7**, 074599–074599 (2013).
- Chowdhury, S., Swenson, B. L., Wong, M. H. & Mishra, U. K. Current status and scope of gallium nitride-based vertical transistors for high-power electronics application. *Semicond. Sci. Technol.* **28**, 074014 (2013).
- Neumayer, D. A. & Ekerdt, J. G. Growth of group III nitrides. A review of precursors and techniques. *Chem. Mater.* **8**, 9–25 (1996).
- Gibart, P. Metal organic vapour phase epitaxy of GaN and lateral overgrowth. *Rep. Prog. Phys.* **67**, 667 (2004).
- Kukushkin, S. *et al.* Substrates for epitaxy of gallium nitride: new materials and techniques. *Rev. Adv. Mater. Sci.* **17**, 1–32 (2008).
- Nakamura, S. GaN growth using GaN buffer layer. *Jpn. J. Appl. Phys.* **30**, L1705 (1991).

12. Amano, H., Sawaki, N., Akasaki, I. & Toyoda, Y. Metalorganic vapor phase epitaxial growth of a high quality GaN film using an AlN buffer layer. *Appl. Phys. Lett.* **48**, 353–355 (1986).
13. Wang, Q. H., Kalantar-Zadeh, K., Kis, A., Coleman, J. N. & Strano, M. S. Electronics and optoelectronics of two-dimensional transition metal dichalcogenides. *Nature Nanotechn.* **7**, 699–712 (2012).
14. Geim, A. K. & Novoselov, K. S. The rise of graphene. *Nature Mater.* **6**, 183–191 (2007).
15. Mak, K. F., Lee, C., Hone, J., Shan, J. & Heinz, T. F. Atomically thin MoS₂: a new direct-gap semiconductor. *Phys. Rev. Lett.* **105**, 136805 (2010).
16. Roy, K. *et al.* Graphene-MoS₂ hybrid structures for multifunctional photoresponsive memory devices. *Nature Nanotech.* **8**, 826–830 (2013).
17. Lopez-Sanchez, O., Lembke, D., Kayci, M., Radenovic, A. & Kis, A. Ultrasensitive photodetectors based on monolayer MoS₂. *Nature Nanotechn.* **8**, 497–501 (2013).
18. Yin, Z. *et al.* Single-layer MoS₂ phototransistors. *ACS Nano* **6**, 74–80 (2011).
19. Perea-López, N. *et al.* Photosensor device based on few-layered WS₂ films. *Adv. Funct. Mater.* **23**, 5511–5517 (2013).
20. Radisavljevic, B., Radenovic, A., Brivio, J., Giacometti, V. & Kis, A. Single-layer MoS₂ transistors. *Nature Nanotechn.* **6**, 147–150 (2011).
21. Kisielowski, C. *et al.* Strain-related phenomena in GaN thin films. *Phys. Rev. B* **54**, 17745 (1996).
22. Kitamura, T., Nakashima, S., Nakamura, N., Furuta, K. & Okumura, H. Raman scattering analysis of GaN with various dislocation densities. *Phys. Status Solidi (c)* **5**, 1789–1791 (2008).
23. Zhao, D., Xu, S., Xie, M., Tong, S. & Yang, H. Stress and its effect on optical properties of GaN epilayers grown on Si (111), 6H-SiC (0001), and c-plane sapphire. *Appl. Phys. Lett.* **83**, 677–679 (2003).
24. Yamada, A., Ho, K., Maruyama, T. & Akimoto, K. Molecular beam epitaxy of GaN on a substrate of MoS₂ layered compound. *Appl. Phys. A* **69**, 89–92 (1999).
25. Yamada, A., Ho, K. P., Takayuki, T., Maruyama, T. & Akimoto, K. Layered compound substrates for GaN growth. *J. Cryst. Growth* **201–202**, 332–335 (1999).
26. Lautenschlager, P., Garriga, M., Logothetidis, S. & Cardona, M. Interband critical points of GaAs and their temperature dependence. *Phys. Rev. B* **35**, 9174 (1987).
27. Li, C., Huang, Y., Malikova, L. & Pollak, F. H. Temperature dependence of the energies and broadening parameters of the interband excitonic transitions in wurtzite GaN. *Phys. Rev. B* **55**, 9251 (1997).
28. Tchounkeu, M., Briot, O., Gil, B., Alexis, J. P. & Aulombard, R.-L. Optical properties of GaN epilayers on sapphire. *J. Appl. Phys.* **80**, 5352–5360 (1996).
29. Rudin, S., Reinecke, T. & Segall, B. Temperature-dependent exciton linewidths in semiconductors. *Phys. Rev. B* **42**, 11218 (1990).
30. Zhang, H., Zhang, Y.-N., Liu, H. & Liu, L.-M. Novel heterostructures by stacking layered molybdenum disulfides and nitrides for solar energy conversion. *J. Mater. Chem. A* **2**, 15389–15395 (2014).

Acknowledgements

The work at TIFR was supported by the Government of India under project 12P0168. S.V., S.R., T.O., V.P., D.J. and H.G.X. acknowledge support from NSF (EFRI-2DARE, Award# 1433490). The authors are thankful to Sandip Ghosh for his valuable help and discussions in PL measurements, and acknowledge the support of B. A. Chalke and R. D. Bapat for help in EBSD measurements. We acknowledge Carina B. Maliakkal and Nirupam Hatui for assistance with materials characterization. We thank Mandar M. Deshmukh for providing bulk MoS₂ crystals for exfoliation.

Author Contributions

P.G. and A.A.R. grew the GaN samples, which were characterized by P.G., S.S. and S.G. synthesized the TMDC materials under the supervision of A.T., and V.P. helped with micro-PL measurements; T.O., S.R. and S.V. provided the TEM results. P.G. and A.B. conceived and designed the study, with inputs from M.R.L., H.G.X. D.J., and P.G. analyzed the data and wrote the manuscript along with A.B. who supervised the entire project.

Additional Information

Supplementary information accompanies this paper at <http://www.nature.com/srep>

Competing financial interests: The authors declare no competing financial interests.

How to cite this article: Gupta, P. *et al.* Layered transition metal dichalcogenides: promising near-lattice-matched substrates for GaN growth. *Sci. Rep.* **6**, 23708; doi: 10.1038/srep23708 (2016).



This work is licensed under a Creative Commons Attribution 4.0 International License. The images or other third party material in this article are included in the article's Creative Commons license, unless indicated otherwise in the credit line; if the material is not included under the Creative Commons license, users will need to obtain permission from the license holder to reproduce the material. To view a copy of this license, visit <http://creativecommons.org/licenses/by/4.0/>

Layered transition metal dichalcogenides: promising near lattice-matched substrates for GaN growth (Supplementary information)

Priti Gupta,^{1, a)} A. A. Rahman,¹ Shruti Subramanian,^{1, b)} Shalini Gupta,^{1, 2} Arumugam Thamizhavel,¹ Tatyana Orlova,³ Sergei Rouvimov,³ Suresh Vishwanath,^{3, c)} Vladimir Protasenko,³ Masihur R. Laskar,⁴ Huili Grace Xing,^{3, c)} Debdeep Jena,^{3, c)} and Arnab Bhattacharya^{1, d)}

¹⁾*Department of Condensed Matter Physics and Materials Science, Tata Institute of Fundamental Research, Mumbai, India*

²⁾*UM-DAE Center for Excellence in Basic Sciences, Mumbai, India*

³⁾*Department of Electrical Engineering, University of Notre Dame, Notre Dame, USA*

⁴⁾*Department of Chemical and Biological Engineering, University of Wisconsin-Madison, USA*

(Dated: 21 January 2016)

^{a)}Presently at Department of Materials Science and Metallurgy, University of Cambridge, Cambridge, UK

^{b)}Presently at Department of Materials Science and Engineering, Pennsylvania State University, Pennsylvania, USA

^{c)}Presently at Department of Electrical and Computer Engineering, Department of Materials Science and Engineering, Cornell University, New York, USA

^{d)}Email: arnab@tifr.res.in

S1. LATTICE PARAMETERS AND BANDGAP VALUES OF TMDCS AND III-NITRIDES

The bandgap versus lattice parameter diagram (Figure 1 of the main manuscript) was plotted based on the room temperature bandgap values of the monolayers of the TMDC materials as available in the literature

III-nitrides

- **AlN:** M. Feneberg, M. F. Romero, B. Neuschl, K. Thonke, M. Röppischer, C. Cobet, N. Esser, M. Bickermann and R. Goldhahn, *Applied Physics Letters* **102** (2013), 052112.
- **GaN:** B. Monemar, *Physical Review B* **10** (1974), 676.
- **InN:** J. Wu, W. Walukiewicz, K. Yu, J. Ager Iii, E. Haller, H. Lu, W. J. Schaff, Y. Saito and Y. Nanishi, *Applied Physics Letters* **80** (2002), 3967–3969.

TMDCs

- **WS₂:** A. Berkdemir, H. R. Gutiérrez, A. R. Botello-Méndez, N. Perea-López, A. L. Elías, C.-I. Chia, B. Wang, V. H. Crespi, F. López-Uriás, J.-C. Charlier *et al.*, *Scientific Reports* **3** (2013).
- **MoS₂, MoSe₂:** S. Tongay, J. Zhou, C. Ataca, K. Lo, T. S. Matthews, J. Li, J. C. Grossman and J. Wu, *Nano letters* **12** (2012), 5576–5580.
- **WSe₂:** P. Tonndorf, R. Schmidt, P. Böttger, X. Zhang, J. Börner, A. Liebig, M. Albrecht, C. Kloc, O. Gordan, D. R. Zahn *et al.*, *Optics express* **21** (2013), 4908–4916.
- **ReSe₂:** C. Ho, P. Liao, Y. Huang, T. Yang and K. Tiong, *Journal of Applied Physics* **81** (1997), 6380–6383.
- **ReS₂:** S. Tongay, H. Sahin, C. Ko, A. Luce, W. Fan, K. Liu, J. Zhou, Y.-S. Huang, C.-H. Ho, J. Yan *et al.*, *Nature Communications* **5** (2014).
- **HfS₂:** D. L. Greenaway and R. Nitsche, *Journal of Physics and Chemistry of Solids* **26** (1965), 1445–1458.
- **TiS₂:** Y.-H. Liu, S. H. Porter and J. E. Goldberger, *Journal of the American Chemical Society* **134** (2012), 5044–5047.
- **ZrS₂:** M. Moustafa, T. Zandt, C. Janowitz and R. Manzke, *Physical Review B* **80** (2009), 035206.

The lattice parameters were obtained from their respective powder diffraction file in the database of Joint Committee on Powder Diffraction Standards (JCPDS), International Center for Diffraction Data, Newtown Square, PA (2013). The following is the list of JCPDS card numbers in the database:

III-nitrides

- **AlN:** 00-025-1133
- **GaN:** 00-050-0792
- **InN:** 00-050-1239

TMDCs

- **WS₂:** 04-003-4478
- **WSe₂:** 00-038-1388
- **MoS₂:** 00-037-1492
- **MoSe₂:** 04-004-8782
- **ReS₂:** 04-002-2231
- **ReSe₂:** 00-050-0537
- **HfS₂:** 00-028-0444
- **ZrS₂:** 00-011-0679
- **TiS₂:** 01-070-6204

S2. PREPARATION OF TRANSITION METAL DICHALCOGENIDES (TMDC) SUBSTRATES

Transition metal dichalcogenides (TMDC) of the type MX_2 where M is a transition metal and X is a chalcogen, are 2D layered materials, with van der Waals forces coupling the layers^{1,2}. They can thus be easily exfoliated into thin monolayer to few-layer sheets, similar to graphene. We first prepared the TMDC crystals by the direct synthesis from their constituent elements. These crystals were exfoliated to get flakes that were transferred to a SiO₂/Si wafer as substrates for GaN growth. In the case of MoS₂, we used naturally available bulk MoS₂ crystals for exfoliation.

A. Crystal growth of TMDCs

A two-step process was followed for the crystal growth of the MX_2 (M= Mo, W, Re and X= S, Se). First the precursors for the crystal growth were prepared by the usual solid-state reaction of a stoichiometric mixture of the respective high purity constituent elements in an evacuated and sealed quartz ampoule ($\sim 10^{-5}$ torr). This quartz ampoule was placed inside a carbolite box furnace, which was slowly ramped to the reaction temperature at the rate of 15 - 20 $^\circ\text{C}/\text{hr}$ and kept at this temperature (1000 - 1200 $^\circ\text{C}$) for 3 - 4 days , then cooled down to room temperature at 50 - 60 $^\circ\text{C}/\text{hr}$. This resulted in flakes of the chalcogenide materials, typically 10 - 100 μm in size being synthesized. This product was then used in a second step to grow single crystals by the iodine vapor transport method. The reacted product (~ 1 g) along with I_2 (150 mg) were inserted in a 20 cm long, cleaned quartz tube, sealed and placed inside a 2-zone furnace. An appropriate temperature gradient ($\sim 100 - 120$ $^\circ\text{C}$) was maintained across the tube for a period of 4-8 days to enable the vapor transport and recrystallization of the material. Temperature parameters and duration during iodine vapor transport of different TMDCs are listed in Table 1.

TABLE I. Temperature parameters and duration during iodine vapor transport of different TMDCs

Initial material	Temperature Distribution		Growth Time (Days)
	Hot Zone ($^\circ\text{C}$)	Cold Zone ($^\circ\text{C}$)	
WS_2	950	850	7
MoS_2	1000	875	7
ReS_2	1020	975	8
WSe_2	800	700	4
MoSe_2	1080	1020	5
ReSe_2	1020	975	8

B. Exfoliation of TMDCs crystals

The TMDCs crystals obtained are then exfoliated using 3M scotch tape and stamped on 300 nm thick SiO_2 -coated Si (~ 1 cm^2). This is then used as a substrate for the growth of GaN. Since our aim was to check the feasibility of the TMDC as a substrate for growth, we did not necessarily optimize the exfoliation to get monolayer sheets.

C. CVD growth of MoS_2

Large area MoS_2 films were synthesized by the vapor phase sulphurization of thin Mo films deposited on sapphire substrates³. Typically $\sim 10 - 15$ nm thick Mo layers were allowed to

react with sulfur in an evacuated and sealed quartz tube at 900-1000 °C for 1 hour. Mo films deposited by sputtering and electron beam evaporation were both used with no significant difference in the quality of the resultant MoS₂.

S3. RAMAN SPECTROSCOPY MEASUREMENT OF MoS₂ AND WS₂ SUBSTRATES

Figure S1 shows the Raman spectra of the bare substrates, which clearly shows two prominent peaks E_{2g}¹ and A_{1g}. The peak positions of these modes indicate the number of layers in the TMDCs^{4,5}. The peak frequencies of E_{2g}¹ and A_{1g} modes correspond to bulk MoS₂, both in case of exfoliated and CVD MoS₂. While in case of WS₂ which is prepared by exfoliating synthesized WS₂ bulk crystal, the number of layers varies from 3 to bulk all over the sample.

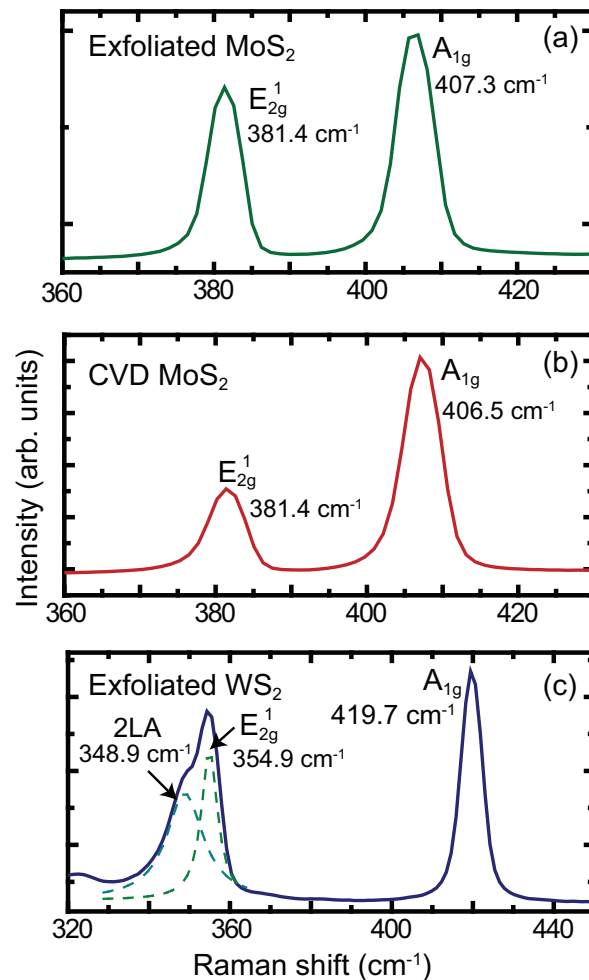


FIG. S1. Raman spectra of bare substrates (a) Exfoliated MoS₂ (b) CVD MoS₂ and (c) exfoliated WS₂ (dashed curves shows the Lorentzian two-peak fit for A_{2g} and 2LA modes).

Figure S2 shows the Raman spectra at different points on the hexagonal flake of GaN/WS₂ reported in Figure 2 of manuscript. It clearly shows the existence of WS₂ across the whole hexagonal flake. The black region between bright areas in the Raman integrated maps of 2LA and A_{1g} modes (Figure 2 of manuscript) are just the regions with relatively low peak intensities. They appear even darker because the colour scale was chosen based on the (more intense) GaN E₂(high) peak.

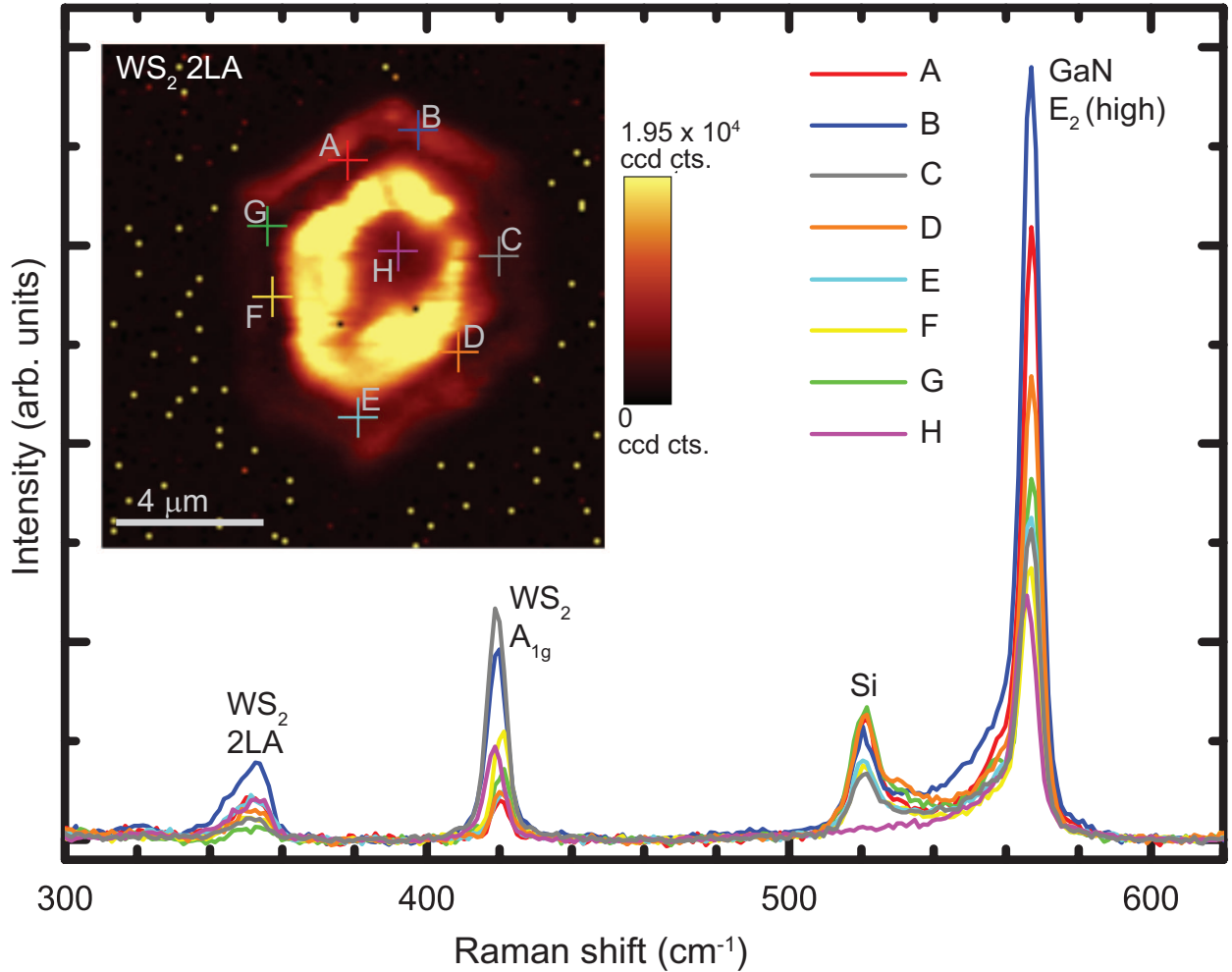


FIG. S2. Raman spectra at different points on the hexagonal flake of GaN/WS₂ reported in Figure 2 of manuscript. It clearly shows existence of WS₂ across the whole flake beneath the GaN.

S4. ANNEALING STUDIES ON MoS₂ AND WS₂

To check the survival of TMDCs in MOVPE growth conditions, we used the mechanically exfoliated TMDCs, which were transferred to 300 nm thick SiO₂-coated silicon wafers, and annealed at different temperatures (700–1040 °C) and in different gas ambients (H₂, NH₃, N₂). Figure S3 shows the representative SEM images of the WS₂ and MoS₂ before and after annealing. While we observed a change in morphology in TMDCs flakes after annealing in NH₃ and H₂ atmosphere, the flakes were intact after annealing at 900 °C in N₂ for 60 s. Also, no characteristic XRD peaks of the corresponding TMDC were observed in the samples, where morphology had changed after annealing. As an example, XRD profile of MoS₂ before and after annealing is shown in Figure S4, where the MoS₂ peaks were not observed after annealing in ammonia at 1040 °C for 60 s, indicating that MoS₂ had degraded while annealing. We believe that at high temperature, H₂ or atomic hydrogen from the decomposition of NH₃ reduces the sulphides to the metal.

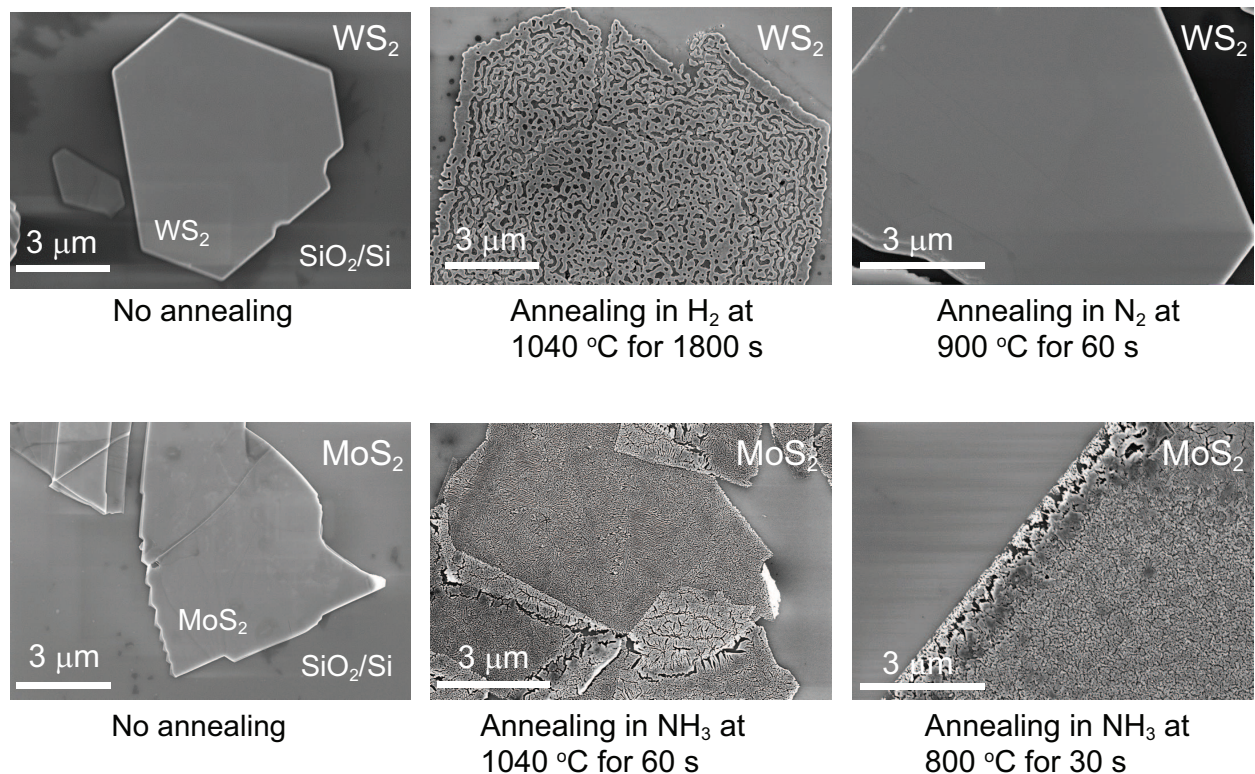


FIG. S3. **Representative SEM images showing the morphology of WS₂ and MoS₂ under different annealing conditions.** Exposure to high temperature, hydrogen and ammonia lead to change of morphology of WS₂ and MoS₂, making MOVPE growth of GaN on TMDCs difficult. However, there is no morphological change on annealing in N₂ at 900 °C for 60 s.

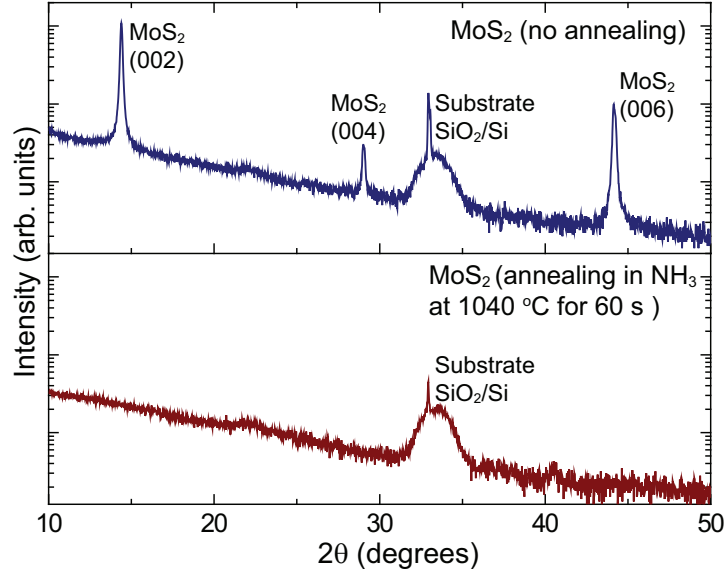


FIG. S4. **XRD profile of MoS₂ before and after exposure to MOVPE growth conditions.** X-ray diffraction shows no characteristic peaks of MoS₂ after annealing in ammonia at 1040 °C for 60 s, indicating degradation of MoS₂ while annealing.

Based on these observations, we optimized our growth conditions for GaN epitaxy on TMDCs. We used N₂ as the carrier gas instead of H₂ gas for ramping up the temperature and switched to H₂ simultaneously with introduction of precursors. An initial nucleation GaN layer was then grown then at 900 °C for 40 s to cover the TMDC layer and hence protect it from further exposure to NH₃ and H₂. Since the GaN layer quality is better at higher temperature, we then ramped up the temperature to 1040 °C for the further growth of GaN on TMDCs. With this procedure, we were able to protect WS₂ layer from degradation after MOVPE growth of GaN, however we need more optimization for the other TMDCs keeping in mind their different thermal stabilities.

S5. ELECTRON BACK SCATTER DIFFRACTION (EBSD) OF GaN/MoS₂

The EBSD map of GaN grown on exfoliated MoS₂ (Figure S5) clearly shows that grown GaN layer is single crystal similar to GaN grown on WS₂ and oriented in (0002) direction.

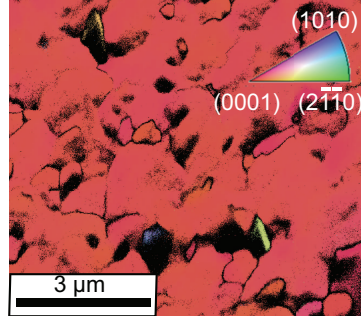


FIG. S5. **EBSD of GaN grown on exfoliated MoS₂** The map shows that GaN layer is single crystal and oriented in (0002) direction

S6. XRD PROFILE OF GaN GROWN ON CVD MoS₂

The XRD profile of GaN grown on CVD MoS₂ is similar to the XRD profile of GaN grown on exfoliated MoS₂.

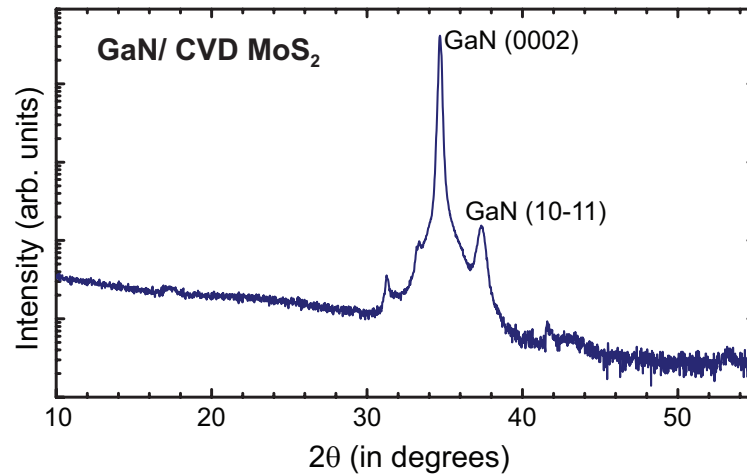


FIG. S6. **XRD profile of GaN layer grown on CVD MoS₂**. It is similar to the GaN layer grown on exfoliated MoS₂ with no substrate peaks observed after the growth.

S7. SECONDARY ION MASS SPECTROMETRY (SIMS) OF GaN GROWN ON CVD MoS₂

As discussed in the main manuscript, MoS₂ was degrading after MOVPE growth of GaN. From an analysis of the behaviour of the photoluminescence of GaN on MoS₂ layers, we surmised that the degradation of MoS₂ left behind sulphur impurities in the layer. This was confirmed from the SIMS profile (done at Evans Analytical Group Inc.) which clearly shows a significant presence of sulphur in the GaN layer (Figure S7).

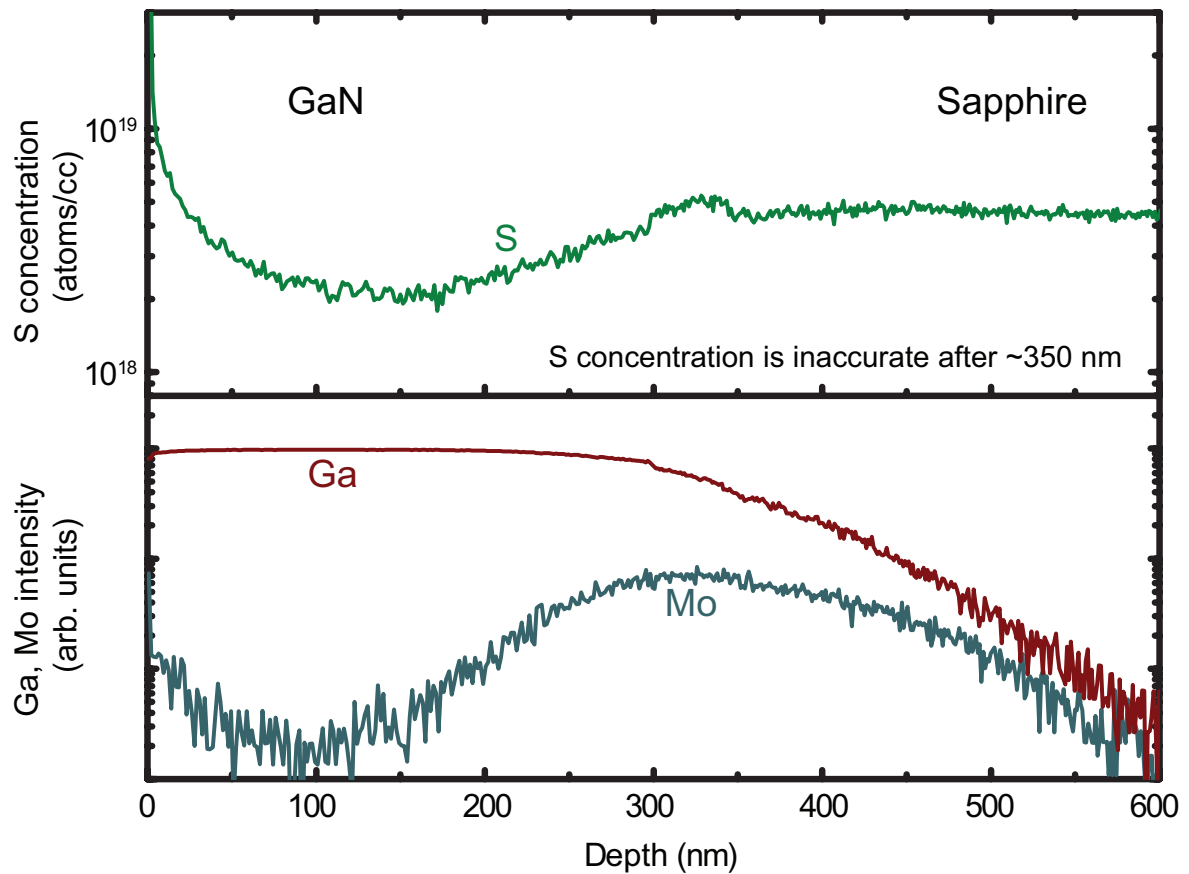


FIG. S7. SIMS profile of GaN grown on CVD MoS₂/sapphire. The profile shows significant presence of sulphur in the GaN layer.

S8. GaN GROWN ON OTHER TMDCs

Growth of GaN layers on other exfoliated TMDCs like WSe₂, MoSe₂, ReS₂ and ReSe₂ was also attempted and Figure S8 shows the corresponding SEM images. All these samples were grown following the same recipe used for the growth of GaN on WS₂ — a short initial layer at 900 °C, followed by 300 s growth at 1040 °C. From the micrographs, it is clear that the growth of GaN is possible on these substrates. However keeping in mind the different thermal stabilities of the various TMDCs, these conditions would need to be optimized independently for each material.

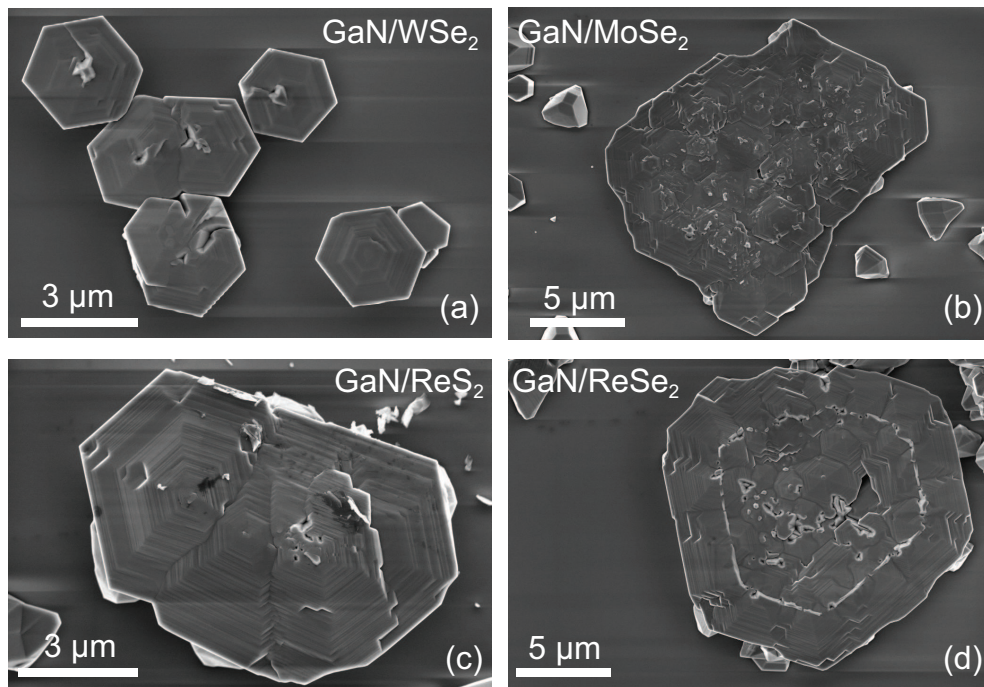


FIG. S8. GaN grown on other TMDCs. SEM images showing GaN grown on (a) WSe₂ (b) MoSe₂ (c) ReS₂ and (d) ReSe₂.

REFERENCES

- ¹Neto, A. & Novoselov, K. New directions in science and technology: two-dimensional crystals. *Rep. Prog. Phys.* **74**, 82501–82509 (2011).
- ²Wang, Q. H., Kalantar-Zadeh, K., Kis, A., Coleman, J. N. & Strano, M. S. Electronics and optoelectronics of two-dimensional transition metal dichalcogenides. *Nature Nanotech.* **7**, 699–712 (2012).
- ³Laskar, M. R. *et al.* Large area single crystal (0001) oriented MoS₂. *Appl. Phys. Lett.* **102**, 252108 (2013).
- ⁴Berkdemir, A. *et al.* Identification of individual and few layers of WS₂ using Raman spectroscopy. *Sci. Rep.* **3** (2013).
- ⁵Li, H. *et al.* From bulk to monolayer MoS₂: evolution of Raman scattering. *Adv. Funct. Mater.* **22**, 1385–1390 (2012).